J Mol Model (2013) 19:5561–5568
DOI 10.1007/s00894-013-2036-0

ORIGINAL PAPER

Theoretical studies of the interaction between influenza virus hemagglutinin and its small molecule ligands

Deshou Song · Hanhong Xu · Shuwen Liu

Received: 20 May 2013 / Accepted: 10 October 2013 / Published online: 21 November 2013

Abstract Hemagglutinin (HA) is a membrane protein present on the influenza viral envelope. It is responsible for molecular recognition between the viral particle and the host cell, as well as fusion of the viral envelope to the endosome bilayer. Because it is essential for influenza viral infection and replication, it has become a target for the design of anti-influenza drugs. Previous studies have identified two small molecule HA ligands (CL-385319 and 1L) that inhibit infection with pseudovirus H5N1 with different potency. In order to compare their different inhibitory activities and shed light on drug design targeting the HA protein, we conducted a variety of theoretical calculations, including docking, molecular dynamics simulations, free energy calculations, as well as quantum calculations to investigate interactions between these two ligands and the HA protein. We found that molecule 1L has stronger π–π interactions with the side chains of residues $F110_2$ and $M24_1$ compared with molecule CL-385319. We propose that these stronger π–π interactions are responsible for the higher inhibitory activity of molecule 1L. Our calculations will aid drug design studies targeting the HA protein.

Keywords Hemagglutinin · Molecular dynamics simulation · MM-GBSA · Quantum calculation · π–π interaction

Electronic supplementary material The online version of this article (doi:10.1007/s00894-013-2036-0) contains supplementary material, which is available to authorized users.

D. Song · H. Xu (✉)
State Key Laboratory for Conservation and Utilization of Subtropical Agro-bioresources, Key Laboratory of Natural Pesticides and Chemical Biology, South China Agricultural University, Guangzhou 510642, China
e-mail: hhxu@scau.edu.cn

S. Liu (✉)
School of Pharmaceutical Sciences, Southern Medical University, Guangzhou 510515, China
e-mail: liusw@smu.edu.cn

Introduction

Hemagglutinin (HA) is a membrane protein present on the influenza viral envelope that mediates molecular recognition between the viral particle and the host cell by binding with sialic acid receptors on the host cell surface. After endocytosis of the viral particle, the HA protein is cleaved into two functional groups known as HA1 and HA2. These two subunits are connected by a single disulfide bond. Acidification of the viral interior induces a variety of conformational changes of the HA2 subunit, as well as fusion of the viral envelope with the endosome membrane. Viral ribonucleoproteins are then released into the host cell and viral replication begins. Therefore, the HA protein is crucial for influenza virus infection and replication. Ligands designed to target the HA protein could inhibit this molecular recognition and membrane fusion, thus preventing viral infection and replication, and have been envisaged as a strategy for treating the influenza pandemic. Broad neutralizing antibodies that recognize the conserved region in the membrane-proximal stem of HA1 and HA2 confer immunity to diverse influenza subtypes [1, 2]. Several small molecules, such as stachyflin [3], BMY-27709 [4], and CL-385319 [5], can block virus infection by inhibiting the low pH-induced conformational change of HA protein required for membrane fusion [4, 6]. Seasonal influenza pandemics currently represent a serious threat to public health, therefore investigations into the HA protein and its ligand interactions could lead to the design of anti-influenza drugs.

Our previous studies have revealed the mechanism of action of CL-385319—a potent inhibitor of the H5N1 influenza virus. CL-385319 inhibits influenza viral infection by binding to the HA protein and preventing molecular recognition between the host cell and the viral particle [7]. Ligand binding of CL-385319 to the HA protein is achieved by the so-called "induced fit" mechanism, where the binding cavity in the receptor adjusts its conformation to accommodate the ligand during the binding process [8]. Our previous calculations found that the following

residues constituted the binding cavity: $V48_2$, $F110_2$, $M24_1$, $E105_2$, $R106_2$, $E103_2$, $T107_2$ and $K51_2$, of which $E105_2$, $T107_2$, $V48_2$, $F110_2$ and $M24_1$ contributed most to the ligand binding free energies. Therefore, these residues were referred to as "hot-spots" in our previous studies [8]. However, Zhu and co-workers have synthesized a series of compounds and found that molecule 1L showed higher inhibitory activity against H5N1 pseudovirus than CL-385319 (IC_{50} values are 0.22 μM and 0.37 μM, respectively) [9]. In order to explain these differences in inhibitory activity, and to compare their binding modes, we conducted a variety of molecular modeling studies to investigate the interactions between these two ligands and the HA protein binding cavity.

We first docked these two compounds individually to the binding site of the HA protein, and calculated the binding free energies using the molecular mechanics generalized Born surface area (MM-GBSA) method. However, we found higher binding affinities of molecule CL-385319 with the protein, which is inconsistent with the experimental IC_{50} values. In order to explain this result, we conducted computational alanine scanning calculations to evaluate interaction strengths between the ligand and different residues in the binding site. We also performed quantum calculations to analyze the noncovalent interactions between ligands and protein as well as the π–π interactions between them. We found that molecule 1L interacts more potently with residues $F110_2$ and $M24_1$, which are crucial for conformational changes in the HA2 protein and for membrane fusion. We propose that these interactions explain the higher inhibitory activity of 1L. Our simulations indicated that not only the binding free energies between ligands and protein but also interactions between ligands and crucial residues in the binding site should be considered in theoretical studies. These results further our understanding of HA–ligand interactions and will aid in the design of novel anti-influenza drugs targeting the HA protein.

Computational methods

Molecular docking and molecular dynamics simulations

The AutoDock package was used to dock molecules CL-385319 and 1L to the binding site of the HA protein. The crystal structure of HA protein (PDB ID: 2IBX) was used in the docking simulations, and 100 independent runs were performed for each molecule. The root mean square deviation (RMSD) values between the docked conformations and the quantum optimized structures were calculated and the conformation with the lowest RMSD value was considered reasonable and used in subsequent calculations.

Molecular dynamics (MD) simulations of a total of 100 ns each were conducted for CL-385315–HA and 1L–HA complexes, respectively. The MD simulations were performed with the AMBER11 [10] package and the structures obtained by docking simulations were used as the initial conformations in the simulations. The restrained electrostatic potential (RESP) charges were calculated for the ligands by the antechamber module of the Amber 11 program following the electronic structure and electrostatic potential calculations at the HF/6-31G* level [11]. The ff99SB force field [12] and the general AMBER force file (GAFF) [13] were used to describe the proteins and ligands, respectively. The complexes were solvated by TIP3P [14] water molecules in a periodic box that extended 8Å from the protein. Na^+ ions were added as counterions to neutralize the simulation systems. The final simulation systems contained the ligand–protein complex, ~27,900 water molecules, and 20 Na^+ ions.

A total of 2,000 steps energy minimization by steepest descent (SD) algorithm were conducted for each system, followed by another 2,000 steps energy minimization using conjugate gradient (CG) algorithm. The energy minimized systems were heated from 1K to 300K in 50 ps steps. Then, another 50 ps MD simulation was conducted with the protein backbone restrained. Finally, a 100-ns MD simulation was performed for each system. All the simulations were conducted under NPT ensemble [15, 16]. The temperature and pressure of the system were maintained at around 300K and 1atm. A time step of 2 f. was used during the simulations.

The structures with the lowest energy during the 100 ns MD simulation were used as reference structures in the RMSD calculations.

Free energy calculations

The MM-GBSA method was used to calculate the binding free energies of the CL-385319–HA and 1L–HA complexes. The binding free energy (ΔG_{bind}) is defined by the following equation:

$$\Delta G_{bind} = G_{com} - G_{rec} - G_{lig} \quad (1)$$

where G_{com}, G_{rec} and G_{lig} are the free energies of the complex, protein, and ligand, respectively. They are defined by the following equation:

$$G = < E_{MM} > + < G_{psolv} > + < G_{npsolv} > - T < S > \quad (2)$$

where E_{MM} is the molecular mechanics energy calculated by sum of the molecular internal energy, the electrostatic interaction energy, and the van der Waals interaction energy; G_{psolv} and G_{npsolv} are the polar and non-polar salvation energies; T represents the temperature of the system, whereas S is the entropy of the molecule.

The nonpolar solvation energy (G_{npsolv}) is calculated based on the solvent accessible surface area (SASA) [17, 18] by the following equation:

$$G_{npsolv} = \gamma \ SASA + b \quad (3)$$

where SASA is determined by the Molsurf method using a probe radius of 1.4 Å. Values of 0.0072 kcal/Å^2 and 0 kcal mol^{-1} were used for γ and b, respectively [19].

Finally, the entropy term was estimated by normal mode analysis of the vibration frequencies of the protein–ligand complex using the nmode module of the AMBER package. The free energy calculations were based on 300 snapshots extracted from the last 30ns of the simulations every 100 ps. The calculated binding free energies of molecules CL-385319 and 1L are listed in Tables 1 and 2, respectively. Although there is still some debate regarding the accuracy of the MM-PBSA and the MM-GBSA methods [20, 21], we show only the results of the MM-GBSA method here.

Computational alanine scanning (CAS) methods [22] were used to calculate the binding free energies of the ligands with HA mutants. In the CAS calculations, a residue in the binding cavity was mutated to alanine and the binding free energy of the ligand-mutated protein complex was computed. Based on the free energies of the wild-type and mutated complexes, the free energy changes (ΔΔG) could be calculated to evaluate the contributions of the mutated residue to the binding free energy. In our studies, we mutated a variety of residues constituting the binding site (listed in Tables 1 and 2) to gain a deeper understanding of the ligand–protein interaction.

Quantum mechanical calculations

To analyze the bonding characteristics of the complexes, the atoms in molecules (AIM) theory of Bader [23, 24] was applied using the AIM 2000 program package [25]. The AIM theory is based on topological analyses of the electron charge densities and their Laplacian values. In the context of quantum calculation of a molecular structure, this theory has proved a valuable tool in defining the concepts of atoms and bonding.

The rigorous AIM theory has been applied successfully to the interpretation of charge densities in a variety of chemical systems [26, 27]. Popelier et al. [28] proposed a set of criteria for the existence of H bonding within AIM formalism. The most prominent evidence of hydrogen bonding is the existence of a bond path between the donor hydrogen nucleus and the acceptor, as well as a bond critical point (BCP) where the electron density (ρ_b) ranges from 0.002 to 0.035 a.u. The AIM calculations in the present study were performed at the B3LYP/6-31 + G (d, p) level.

Results and discussion

Molecular docking

The AutoDock program was used to dock the compounds to the binding site of the HA protein (PDB ID: 2IBX). For each molecule, 100 independent runs were conducted. The conformations generated by docking simulations were compared with the structures optimized by quantum calculations, and the conformations with lowest RMSD values were chosen and used in subsequent MD simulations. Superimposition of the quantum optimized structures and the docked structures are shown in Fig. 1. The all atom RMSD values of CL-385319 and 1L were 1.46Å and 0.95 Å, respectively. The relatively large structural differences

Table 1 Free energy calculation (kcal mol^{-1}) of CL-385319 binding to wild-type and the mutated hemagglutinin (HA) protein

	Energy terms (kcal mol^{-1})[a]				ΔG (kcal mol^{-1})	ΔΔG (kcal mol^{-1})
	ΔE_{vdw}	ΔE_{ele}	$\Delta G_{psolv\ v}$	ΔG_{npsol}		
Wild-type	−32.3	−17.8	23.6	−4.8	−31.2	—
$R106_2$	−30.4	−19.7	28.4	−4.6	−26.3	4.9
$E103_2$	−31.4	−15.3	20.0	−4.6	−31.2	0.0
$H111_2$	−32.2	−17.8	23.4	−4.7	−31.2	0.0
$L2_2$	−30.7	−17.9	23.7	−4.6	−29.4	1.7
$K51_2$	−31.7	−19.4	25.8	−4.7	−29.9	1.3
$M24_1$	−28.9	−17.3	23.0	−4.1	−27.3	3.9
$F110_2$	−28.1	−17.5	23.2	−4.2	−26.6	4.6
$T107_2$	−31.8	−17.7	24.6	−4.7	−29.6	1.6
$V48_2$	−32.2	−17.8	23.6	−4.7	−31.06	0.1
$\sum_{HS}$ [b]	—	—	—	—	—	10.3
$\sum_{M24_1+F110_2}$ [c]	—	—	—	—	—	8.5

[a] ΔE_{vdw}, ΔE_{ele}, ΔG_{psolv}, ΔG_{npsolv} are the free energy changes of the van der Waals interaction energies, the electrostatic interaction energies, the polar salvation energies, as well as the non-polar salvation energies, respectively

[b] $\sum_{HS}$ represents the sum of the free energy changes (ΔΔG) upon mutations of $M24_1$, $F110_2$, $T107_2$ and $V48_2$

[c] $\sum_{M24_1+F110_2}$ represents the sum of the free energy changes (ΔΔG) upon mutations of $M24_1$ and $F110_2$

Table 2 Free energy calculation (kcal mol^{-1}) of molecule 1L binding to wild-type and the mutated HA protein[a]

	Energy terms (kcal mol^{-1})				ΔG (kcal mol^{-1})	ΔΔG (kcal mol^{-1})
	ΔE_{vdw}	ΔE_{ele}	$\Delta G_{psolv\ v}$	ΔG_{npsol}		
Wild-type	−33.7	−4.4	19.1	−4.7	−23.7	—
$R106_2$	−32.7	0.0	14.5	−4.6	−22.8	0.9
$E103_2$	−33.4	−2.4	17.6	−4.7	−22.9	0.7
$H111_2$	−32.9	−4.8	19.8	−4.7	−22.5	1.2
$L2_2$	−32.8	−4.4	19.2	−4.7	−22.7	1.0
$K51_2$	−32.2	−6.2	20.2	−4.5	−22.8	0.9
$M24_1$	−30.4	−4.1	18.8	−4.2	−20.0	3.7
$F110_2$	−28.5	−3.7	19.7	−4.3	−16.8	6.9
$T107_2$	−33.1	−3.4	18.4	−4.6	−22.8	0.9
$V48_2$	−33.7	−4.4	19.1	−4.7	−23.7	0.0
$\sum_{HS}$b	—	—	—	—	—	11.5
$\sum_{M24_1+F110_2}$[c]	—	—	—	—	—	10.6

[a] All definitions as in Table 1

between the quantum optimized structure and the docked structure are reasonable because the conformations of the ligands are changed to fit to binding cavity of the HA protein. The interaction details between these two molecules and the receptor revealed by docking simulations are shown in Fig. 2.

Molecular dynamics simulations and free energy calculations

Our MD simulations found that the initial structures of both ligand–HA complexes were stable throughout the entire simulation time. The two ligands showed very similar binding conformations at the binding site. For instance, the "induced fit" mechanism revealed in our previous simulations of the CL-385319–HA complex [8] was also found in simulations of the 1L–HA complex, with the benzene ring of the ligand sandwiched between residues $F110_2$ and $M24_1$ in both complexes. In our previous simulations of the CL-385319–HA complex [8], a hydrogen bond between ligand and the $V48_2$ residue was broken during the "induced fit" process. Similar interactions were also found in simulations of the 1L-HA complex, as shown in Movie SI (Supplemental data, Movie SI).

In order to further investigate the interactions between ligands (CL-385319 and 1L) and the HA protein, 100-ns MD simulations were conducted for the CL-385319–HA and 1L–HA complexes. The binding free energies of these two molecules at the HA binding cavity were then calculated by the MM-GBSA method based on 300 snapshots extracted from the last 30 ns of the dynamics simulations (Fig. 3). The

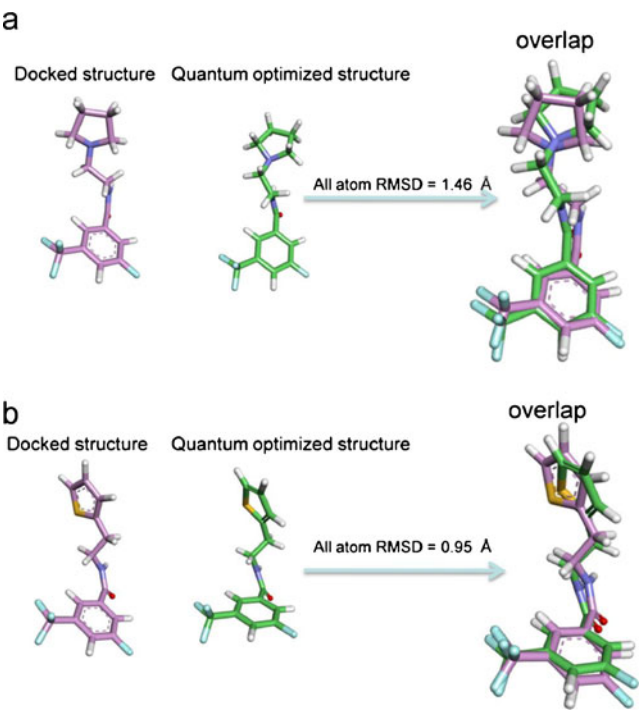

Fig. 1 Quantum optimized molecular structures (*magenta*) and docked conformations (*cyan*) with lowest root mean square deviation (RMSD) values of CL385319 (**a**) and 1L (**b**)

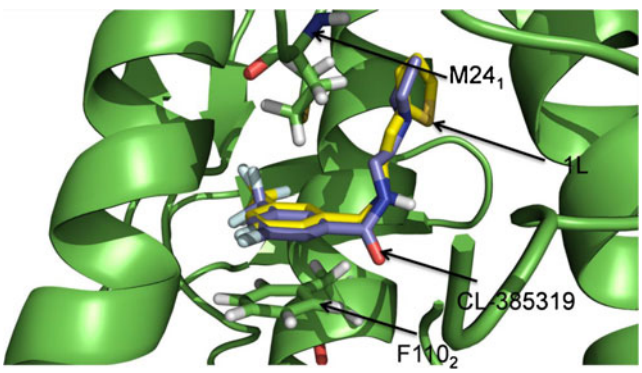

Fig. 2 Binding conformations obtained by molecular docking simulations of molecules CL-385319 and 1L at the binding cavity of hemagglutinin (HA) protein

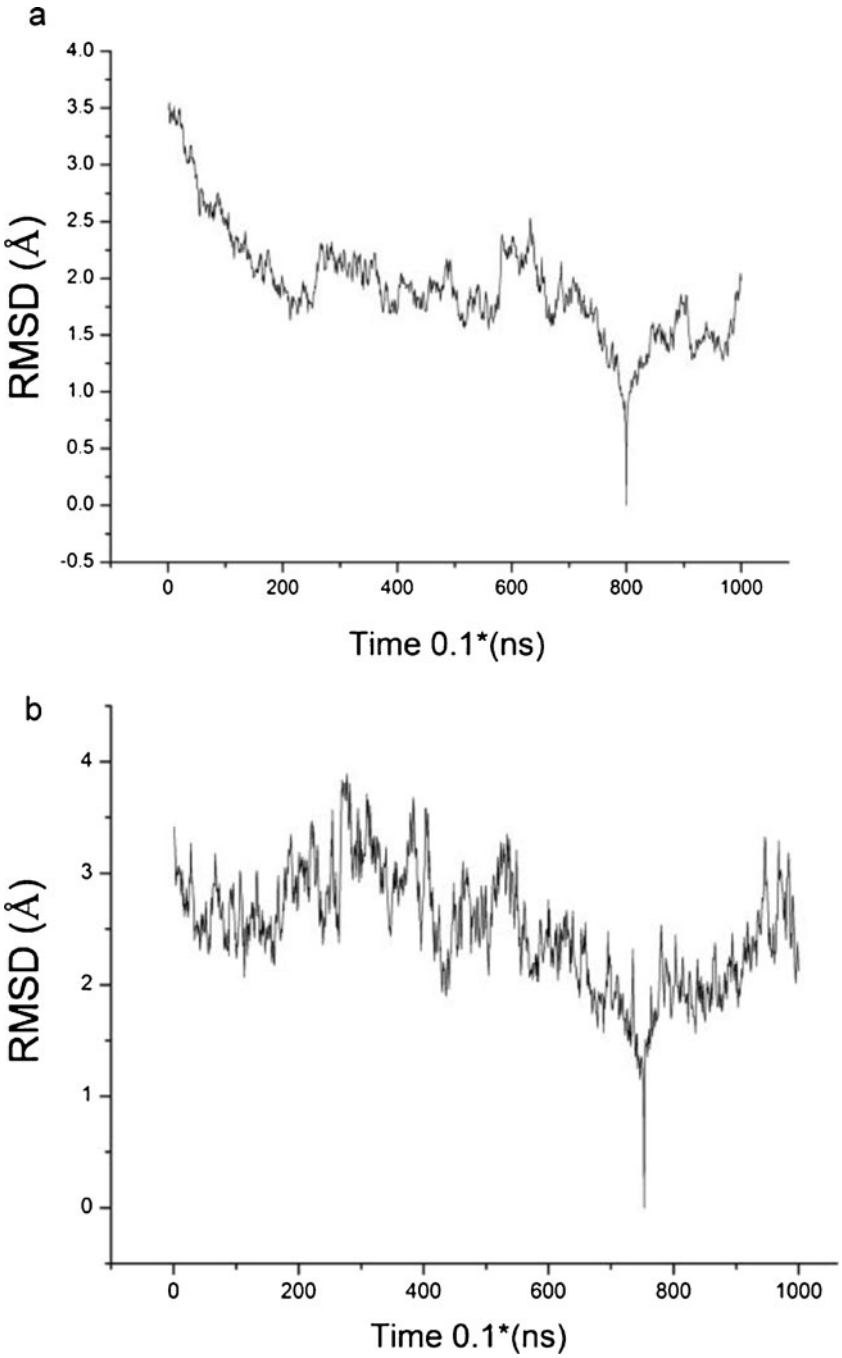

Fig. 3 Root mean square deviation (RMSD) values of the protein backbone of the CL-385315-HA (**a**) and 1L-HA (**b**) complexes during MD simulations

binding free energies were −31.2 kcal mol^{-1} and −23.7 kcal mol^{-1} for CL-385319 and 1L, respectively. The lower binding free energy of CL-385319 may imply higher binding affinity of CL-385319 with the HA protein, which is inconsistent with the experimental results that 1L is a more potent inhibitor of the H5N1 pseudovirus [9].

To try to resolve this apparent conflict, we employed the CAS method to evaluate the contributions of residues at the binding site to binding free energies. In the CAS calculations, residues in the binding site were mutated to alanine residues and the free energy changes (ΔΔG) upon mutations were calculated. Mutations that resulted in free energy changes larger than 1 kcal mol^{-1} were considered crucial for ligand binding. According to the free energy calculation results in Tables 1 and 2, residues $K51_2$, $L2_2$, $R106_2$, $T107_2$, $F110_2$ and $M24_1$ were crucial for CL-385319-HA binding, whereas residues $H111_2$, $M24_1$ and $F110_2$ were crucial for 1L-HA binding. Our previous study confirmed that CL-385319 was sandwiched by $F110_2$ and $M24_1$ via π–π interactions [8]. Combining the free energy changes (ΔΔG) upon mutations in Tables 1 and 2, we found that values were 10.3 kcal mol^{-1} and 11.5 kcal mol^{-1}, respectively, for CL-385319 and 1L.

When considering only residues $F110_2$ and $M24_1$, the sum of free energy changes ($\Delta\Delta G$) were 8.5 kcal mol^{-1} and 10.6 kcal mol^{-1}, respectively, for CL-385319 and 1L. Larger $\Delta\Delta G$ values indicate stronger interactions between ligands and these residues. Therefore, 1L has stronger interactions with residues constituting the binding cavity (particularly $F110_2$ and $M24_1$) than CL-385319. $F110_2$ and $M24_1$ are the most important residues in the binding cavity, because their mutation causes the loss of inhibitory activity of CL-395319 against H5N1 pseudovirus infection. We propose that the stronger interactions between 1L and these two residues make 1L more potent than CL-385319.

Quantum calculations reveal stronger interactions between molecule 1L and crucial residues at the binding cavity

In order to further compare the strengths of the interactions between these two ligands and the HA protein, we conducted quantum calculations to evaluate the noncovalent contacts and π–π interactions between them. The charge densities of BCPs were calculated based on the conformation with the lowest energy during the MD simulations; the results are listed in Table 3. The noncovalent interactions between the ligands and residues at the binding site found in our calculations are shown in Table 3 [29]. A total of 25 noncovalent interactions was found between molecule 1L and the binding site, whereas only 23 noncovalent interactions were found between molecule CL-385319 and the binding cavity. Counting only the interactions between the ligands and residues $T107_2$, $F110_2$ and $M24_1$, the number of nocovalent interactions were 15 and 9, respectively, for molecules 1L and CL-385319 (Table 3, Figure S1–S18). These results suggest that 1L has stronger interactions with $T107_2$, $F110_2$ and $M24_1$ than CL-385319, thus explaining the higher inhibitory activity of molecule 1L [29].

Arene–arene interactions play an essential role in the interaction between ligand and protein [30–32]. The benzene ring of molecule CL-385319 was sandwiched by $F110_2$ and $M24_1$ side chains via π–π interactions, and the charge density of case saddle point was 0.0005 a.u., which is very weak (Fig. 4). However, the charge

Table 3 Noncovalent Interactions, charge densities (ρ_b) and their Laplacian ($\nabla^2\rho_b$) at bond critical points (BCPs) between substrates and main residues at B3LYP/6-31 + G (d,p) level (a.u.)

Noncovalent bond	Charge density (ρ_b)	Laplacia ($\nabla^2\rho_b$)	Noncovalent bond	Charge density (ρ_b)	Laplacia ($\nabla^2\rho_b$)
1L-A44-1: C-H…O	0.0021	0.0088	CL-385319-R106-1: C-H…π	0.0040	0.0121
1L-R106-1: C-H…H-C	0.0023	0.0077	CL-385319-R106-2: C-H…H-C	0.0046	0.0165
1L-R106-2: C-H…O	0.0043	0.0157	CL-385319-R106-3: C-H…π	0.0112	0.0367
1L-G47-1: C-H…π	0.0028	0.0082	CL-385319-R106-4: C-H…H-C	0.0036	0.0118
1L-G47-2: C-H…S	0.0070	0.0295	CL-385319-E103-1: C-H…O	0.0029	0.0111
1L-H111-1: C-H…π	0.0026	0.0086	CL-385319-E103-2: O…π	0.0025	0.0098
1L-K51-1: C-H…H-C	0.0036	0.0121	CL-385319-E103-3: C-H…H-C	0.0040	0.0145
1L-K51-2: C-H…S	0.0081	0.0267	CL-385319-E103-4: C-H…H-C	0.0032	0.0111
1L-M24-1: C-H…S	0.0031	0.0098	CL-385319-E105-1: C-H…π	0.0031	0.0114
1L-M24-2: C-H…π	0.0039	0.0114	CL-385319-G1-1: N-H…O	0.0061	0.0250
1L-M24-3: C-S…π	0.0041	0.0105	CL-385319-G1-2: C-H…O	0.0054	0.0215
1L-M24-4: C-H…O	0.0028	0.0110	CL-385319-I23-1: C-H…H-C	0.0039	0.0142
1L-F110-1: C-H…H-C	0.0039	0.0139	CL-385319-I23-2: C-H…H-C	0.0035	0.0120
1L-F110-2: C-H…H-C	0.0082	0.0313	CL-385319-L2-1: C-H…O	0.0053	0.0190
1L-F110-3: π…π	0.0045	0.0124	CL-385319-M24-1: C-H…H-C	0.0073	0.0232
1L-F110-4: π…π	0.0037	0.0102	CL-385319-M24-2: C-H…S	0.0123	0.0335
1L-F110-5: π…π	0.0063	0.0166	CL-385319-M24-3: C-S…π	0.0094	0.0297
1L-F110-6: C-H…F	0.0048	0.0216	CL-385319-M24-4: C-H…π	0.0034	0.0111
1L-T107-1: C-H…O	0.0125	0.0402	CL-385319-F110-1: C-F…π	0.0070	0.0263
1L-T107-2: C-H…H-C	0.0064	0.0256	CL-385319-F110-2: C-F…π	0.0070	0.0269
1L-T107-3: C-H…H-C	0.0040	0.0149	CL-385319-F110-3: π…π	0.0063	0.0168
1L-T107-4: C-H…O	0.0022	0.0090	CL-385319-T107-1: C-H…π	0.0026	0.0076
1L-T107-5: C-H…π	0.0056	0.0177	CL-385319-T107-2: C-H…O	0.0044	0.0156
1L-V48-1: C-H…π	0.0059	0.0191			
1L-V48-2: C-H…π	0.0048	0.0142			

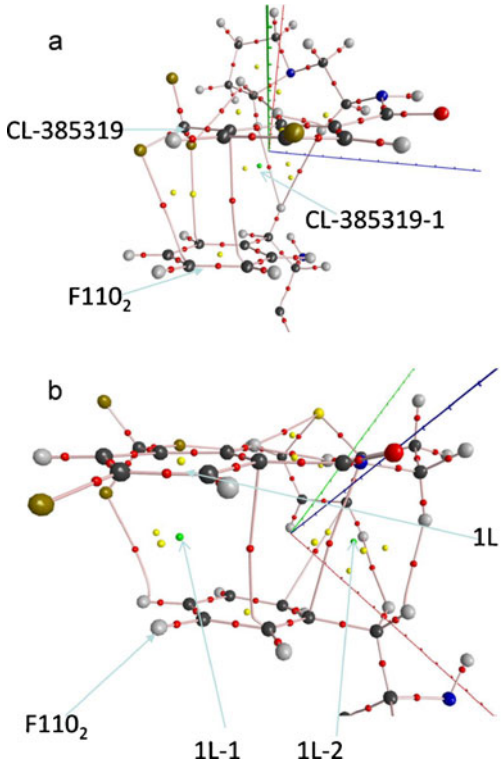

Fig. 4 Noncovalent interactions between residue F110$_2$ and CL-385319 (**a**) or 1L (**b**). CL-385319-1, 1L-1 and 1L-2 are case saddle points

densities of two case saddle points 1L-1 and 1L-2 were 0.0037 a.u. and 0.0017 a.u., respectively, which are much stronger than that of CL-385319-1 (Fig. 4b). These calculations indicate stronger π–π interactions in the 1L–HA complex than in the CL-385319–HA complex. The C-X···π (X = H, S or F) interactions and C-H···H-C interactions are also crucial noncovalent interactions between ligands and the residues constituting the binding cavity of the HA protein except for the π–π interactions, as shown in Table 3.

Conclusions

Hemagglutinin (HA) is a membrane protein on the influenza viral envelope that mediates membrane fusion of the viral membrane with the endosome bilayer during infection with influenza virus. Therefore, design HA inhibitors that could prevent recognition between viral particle and host cell has been used as a strategy for treating influenza virus infection. In this study, we conducted a variety of theoretical studies to compare the interactions between two structurally related HA inhibitors, CL-385319 and 1L, and the HA protein.

Theoretical calculations have proved a reliable method with which to investigate ligand–protein interactions and protein–protein interactions [33–35]. Free energy calculations based on the MM-GBSA method revealed higher binding affinities between molecule CL-385319 and the HA protein, which is inconsistent with its lower inhibitory activity for H5N1 pseudovirus. To reconcile this controversy, we calculated the contributions of crucial residues in the binding cavity to the free energy using the CAS method, and found that 1L interacted more potently with residues F110$_2$ and M24$_1$. Quantum calculations also revealed much stronger π–π interactions between the benzene ring of 1L and side chains of residues F110$_2$ and M24$_1$. These results may explain the higher inhibitory activity of molecule 1L for the H5N1 pseudovirus.

An important conclusion of our calculations is that the interactions between the inhibitors and several crucial residues at the binding cavity are highly corelated with their inhibitory potency. Therefore, in future drug design studies, these interactions should be considered carefully in order to improve ligands activity. Our research illustrates that the interactions between HA and its small molecule ligands may lead to possible anti-influenza drug design in the future.

Acknowledgments This work was supported by the Natural Science Foundation of China (30772602), the foundation from Key Laboratory of Prevention and Control of Emerging Infectious Diseases of Guangdong Higher Education Institutes (KLB09007), the Guangdong Pearl River Scholar Funded Scheme to S.L. and H.X., High-level Personnel Project Foundation of Guangdong Province to S.L. and H.X.

Competing interests The authors have declared that no competing interests exist.

References

1. Harrison SC (2008) Viral membrane fusion. Nat Struct Mol Biol 15: 690–698
2. Reed ML, Bridges OA, Seiler P et al (2010) The pH of activation of the hemagglutinin protein regulates H5N1 influenza virus pathogenicity and transmissibility in ducks. J Virol 84:1527–1535
3. Yoshimoto J, Kakui M, Iwasaki H et al (1999) Identification of a novel HA conformational change inhibitor of human influenza virus. Arch Virol 144:865–878
4. Luo G, Colonno R, Krystal M (1996) Characterization of a hemagglutinin-specific inhibitor of influenza A virus. Virology 226: 66–76
5. Plotch SJ, O'Hara B, Morin J et al (1999) Inhibition of influenza A virus replication by compounds interfering with the fusogenic function of the viral hemagglutinin. J Virol 73:140–151
6. Luo G, Torri A, Harte WE et al (1997) Molecular mechanism underlying the action of a novel fusion inhibitor of influenza A virus. J Virol 71:4062–4070
7. Liu S, Li R, Zhang R et al (2011) CL-385319 inhibits H5N1 avian influenza A virus infection by blocking viral entry. Eur J Pharmacol 660:460–467
8. Li R, Song D, Zhu Z et al (2012) An induced pocket for the binding of potent fusion inhibitor CL-385319 with H5N1 influenza virus hemagglutinin. PLoS One 7:e41956

9. Zhu Z, Li R, Xiao G et al (2012) Design, synthesis and structure-activity relationship of novel inhibitors against H5N1 hemagglutinin-mediated membrane fusion. Eur J Med Chem 57:211–216
10. Case DA, Darden TA, Cheatham TE et al (2011) AMBER11. University of California, San Francisco
11. Frisch MJ, Trucks GW, Schlegel HB et al (2010) Gaussian 09. Revision B.01 ed. Gaussian, Wallingford
12. Lindorff-Larsen K, Piana S, Palmo K et al (2010) Improved side-chain torsion potentials for the Amber ff99SB protein force field. Proteins 78:1950–1958
13. Ozpinar GA, Peukert W, Clark T (2010) An improved generalized AMBER force field (GAFF) for urea. J Mol Model 16:1427–1440
14. Price DJ, Brooks CL III (2004) A modified TIP3P water potential for simulation with Ewald summation. J Chem Phys 121:10096–10103
15. Taylor J, Whiteford NE, Bradley G et al (2009) Validation of all-atom phosphatidylcholine lipid force fields in the tensionless NPT ensemble. Biochim Biophys Acta 1788:638–649
16. Bosko JT, Todd BD, Sadus RJ (2005) Molecular simulation of dendrimers and their mixtures under shear: comparison of isothermal-isobaric (NpT) and isothermal-isochoric (NVT) ensemble systems. J Chem Phys 123:34905
17. Dunn WJ 3rd, Koehler MG, Grigoras S (1987) The role of solvent-accessible surface area in determining partition coefficients. J Med Chem 30:1121–1126
18. Richmond TJ (1984) Solvent accessible surface area and excluded volume in proteins. Analytical equations for overlapping spheres and implications for the hydrophobic effect. J Mol Biol 178:63–89
19. Connolly ML (1983) Analytical molecular surface calculation. J Appl Crystallogr 548–558
20. Rastelli G, Del Rio A, Degliesposti G et al (2010) Fast and accurate predictions of binding free energies using MM-PBSA and MM-GBSA. J Comput Chem 31:797–810
21. Hou T, Wang J, Li Y et al (2011) Assessing the performance of the MM/PBSA and MM/GBSA methods. 1. The accuracy of binding free energy calculations based on molecular dynamics simulations. J Chem Inf Model 51:69–82
22. Kortemme T, Kim DE, Baker D (2004) Computational alanine scanning of protein-protein interfaces. Sci STKE 2004:pl2
23. Bader R (1994) Atoms in molecules, a quantum theory. Department of Chemistry, McMaster University, Ontario, Canada. Clarendon, Oxford
24. Koch U, Popelier PLA (1995) Characterization of C–H–O hydrogen bonds on the basis of the charge density. J Phys Chem 99:9747–9754
25. Biegler-König F, Schönbohm J, Derdau R et al (2002) AIM 2000. Version 2.0 edn. McMaster University, Hamilton, Canada
26. Louit G, Hoquet A, Ghomi M et al (2002) Are guanine tetrads stabilised by bifurcated hydrogen bonds: an AIM topological analysis of electron density. PhysChemComm 94–98
27. Louit G, Hoquet A, Ghomi M et al (2002) Guanine tetrads interacting with metal ions. An AIM topological analysis of the electron density. PhysChemComm 1–5
28. Popelier P (1998) Characterization of a dihydrogen bond on the basis of the electron density. J Phys Chem A 102:1873–1878
29. Salonen LM, Ellermann M, Diederich F (2011) Aromatic rings in chemical and biological recognition: energetics and structures. Angew Chem Int Ed Engl 50:4808–4842
30. Burley SK, Petsko GA (1988) Weakly polar interactions in proteins. Adv Protein Chem 39:125–189
31. Burley SK, Petsko GA (1985) Aromatic–aromatic interaction: a mechanism of protein structure stabilization. Science 229:23–28
32. Meyer EA, Castellano RK, Diederich F (2003) Interactions with aromatic rings in chemical and biological recognition. Angew Chem Int Ed Engl 42:1210–1250
33. Zhou R, Das P, Royyuru AK (2008) Single mutation induced H3N2 hemagglutinin antibody neutralization: a free energy perturbation study. J Phys Chem B 112:15813–15820
34. Das P, Li J, Royyuru AK et al (2009) Free energy simulations reveal a double mutant avian H5N1 virus hemagglutinin with altered receptor binding specificity. J Comput Chem 30:1654–1663
35. Xia Z, Huynh T, Kang SG et al (2012) Free-energy simulations reveal that both hydrophobic and polar interactions are important for influenza hemagglutinin antibody binding. Biophys J 102:1453–1461